S = 1 Tetraazacyclophane Diradical Dication with Robust Stability: a Case of Low Temperature One-Dimensional Antiferromagnetic Chain

Wenqing Wang,[†] Chao Chen,[†] Chan Shu,[‡] Suchada Rajca,[‡] Xinping Wang,*[,†] Andrzej Rajca*[,‡]

[†]State Key Laboratory of Coordination Chemistry, School of Chemistry and Chemical Engineering, Collaborative Innovation Center of Advanced Microstructures, Nanjing University, Nanjing 210023, China

[‡]Department of Chemistry, University of Nebraska, Lincoln, Nebraska 68588, USA

ABSTRACT: One-dimensional (1-D) spin-1 (S = 1) chain of organic radicals with low local magnetic anisotropy may provide a better understanding of the low-dimensional magnetism. We report solid-state studies, including single crystal X-ray crystallography, of an air-stable tetraazacyclophane diradical dication salt $\mathbf{1}^{2\cdot 2+}\cdot 2[Al(OC(CF_3)_2CH_3)_4]^-$ with a triplet ground state ($\Delta E_{ST} \approx 0.5$ kcal mol^{-1}). The magnetic behavior for $\mathbf{1}^{2\cdot 2+}$ at low temperature is best modeled by 1-D spin S = 1 Heisenberg chain with intrachain antiferromagnetic coupling of J'/k = −5.4 K, which is associated with the inter-aryl C···C contacts, including π-π interactions. Zero-field splitting value, $|D/hc| \approx 5.6 \times 10^{-3}$ cm^{-1}, for $\mathbf{1}^{2\cdot 2+}$ is rather small, and thus the 1-D chains are characterized by the high degree of isotropicity $|D/2J| \approx 7.5 \times 10^{-4}$. The diradical dication salt possesses extraordinary stability with onset of decomposition at temperature of about 180 °C (~450 K), based on thermogravimetric analysis and EPR spectroscopy.

INTRODUCTION

Low-dimensional spin systems have remarkably enhanced quantum fluctuations to give rise to various strongly correlated states and enable the appearance of multiple quantum phases with unique characteristics.[1] They are important not only for the discovery of novel quantum states of matter, but also a superb tool for testing various theoretical concepts.[1] One of the most fundamental low-dimensional spin models of quantum magnetism is represented by the isotropic S = 1 Heisenberg antiferromagnetic chain in which the Haldane's conjecture[2] has inspired numerous theoretical studies of integer spins (primarily S = 1) in low dimensions.[3] The Haldane gap, the energy gap between the singlet spin-liquid ground state and the lowest excited state (S =1 triplet),[2] has been experimentally confirmed in some 1-D spin S = 1 quantum magnets based on transition metal complexes.[4] However, characterization of the spin excitation spectrum in such systems has not been achieved, because the Haldane phase is effectively destroyed by the interactions of the single ion anisotropy and inter-chain coupling.[4d] Organic magnetic chains with S = 1 local spins (Scheme 1) are expected to possess much lower local magnetic anisotropy and thus are best suited to understand the low-dimensional magnetism.

Scheme 1. Schematic Presentation of the Antiferromagnetic Chain of S = 1 Diradicals

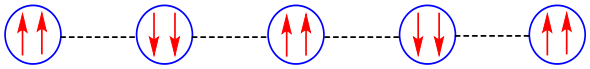

Stable organic diradicals have received a considerable attention owing to their intriguing solid-state properties.[5] While a number of stable triplet ground state (S = 1) diradicals with strong ferromagnetic coupling have been prepared,[6-9] only a single case of 1-D antiferromagnetic spin-1 chains based on triplet diradicals has been reported. In 2007, Rajca and coworkers reported two 1-D chains of S = 1 neutral nitroxide diradicals featuring intra-chain antiferromagnetic coupling.[8a] The formation of the 1-D spin chains were associated with the methyl-nitroxide C-H···O contacts, including nonclassical hydrogen bonds, thus the intra-chain coupling constant $J'/k \approx -3$ K was relatively weak (Figure 1).[8]

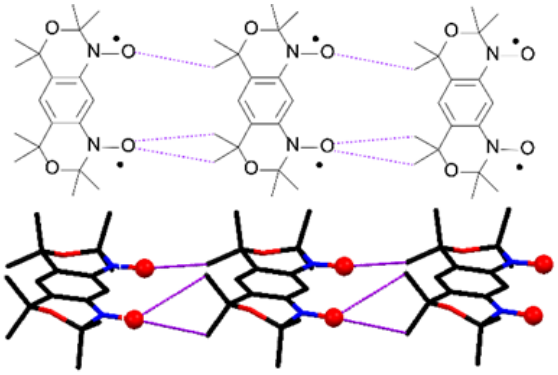

Figure 1. 1-D chains of S = 1 nitroxide diradicals: the methyl-nitroxide C-H···O contacts are indicated in purple color.

Tetraaza[1.1.1.1]*m*,*p*,*m*,*p*-cyclophane diradical dication ($\mathbf{1}^{2\cdot 2+}$) was reported as a triplet diradical.[9a] Its unique magnetic and redox properties have attracted great attention as potential building blocks for the development of molecular electronics. Considerable efforts

have been made to explore various azacyclophanes structures,[10] including the very recent reinvestigation of derivatives of $\mathbf{1}^{2\cdot 2+}$ by Ito[7a] and Wang.[7b] The crystallographic characterization of azacyclophane-based diradical dications not only affirms their superior stability, but also provided better insight into the magnetic properties. Notably, none of these studies revealed the intriguing magnetic properties related to low-dimensional spin systems. Also, thermal stability of the diradical dication and its derivatives, to our knowledge, has not been investigated.

Here we disclose a 1-D antiferromagnetic chain of $S = 1$ diradical dication $\mathbf{1}^{2\cdot 2+}$ that consists of intra-chain aryl C···C contacts arising from π-π interactions and exhibits a relatively strong intra-chain coupling constant $J'/k = -5.4$ K. The $S = 1$ anisotropy in $\mathbf{1}^{2\cdot 2+}$ is low, as measured by the zero-field splitting value $|D/hc| \approx 5.6 \times 10^{-3}$ cm^{-1}, compared to $|D/hc| = 1.350 \times 10^{-2}$ cm^{-1} in the previously studied nitroxide diradical.[8] Hence, the resultant 1-D antiferromagnetic spin-1 chains are characterized by the unprecedented high degree of isotropicity $|D/2J| \approx 7.5 \times 10^{-4}$. We carried out thermal gravimetric analysis (TGA) to show that the diradical dication salt possesses extraordinary stability with onset of decomposition at temperature of about 180 °C (~450 K).

RESULTS AND DISCUSSION

Preparation of the Diradical Dication. Tetraazacyclophane **1** was synthesized according to the literature procedure[9a] and characterized by NMR spectroscopy. Considering its solid-state structure was unknown, our goal was to obtain crystals of the tetraazacyclophane diradical dication $\mathbf{1}^{2\cdot 2+}$ for further studies. Because the polyfluoroalumate anion such as $[Al(OR_{Me})_4]^-$ (OR_{Me} = $OC(CF_3)_2Me$) is known to robustly stablize and crystallize diradical dications,[11] we reacted **1** with two equivalents of $Ag[Al(OR_{Me})_4]$[12] in CH_2Cl_2, to provide diradical dication salt $\mathbf{1}^{2\cdot 2+}\cdot 2[Al(OR_{Me})_4]^-$ in a good yield (Scheme 2). The salt was thermally stable and may be exposed to the air for several weeks at room temperature.

Scheme 2. The 2e-Oxidation Reaction of 1 Leading to the Formation of Diradical Dication Salt $\mathbf{1}^{2\cdot 2+}\cdot 2[Al(OR_{Me})_4]^-$

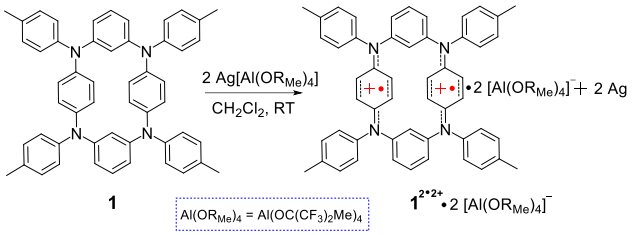

X-ray Crystallography and Molecular Modeling. Single crystals suitable for X-ray crystallographic studies were obtained by cooling the $\mathbf{1}^{2\cdot 2+}\cdot 2[Al(OR_{Me})_4]^-$ solution in CH_2Cl_2 (Table S1, SI).[13] The molecular structure of $\mathbf{1}^{2\cdot 2+}$ is illustrated as Ortep plots in Figure 2. The closest inter-aryl C···C distance is 3.68 Å (C18···C19') between para-bridged aryl rings. Two *para*-bridged aryl rings are nearly orthogonal with the dihedral angle of 75.5°, forming an exchange coupling pathway for an intramolecular ferromagnetic coupling in $\mathbf{1}^{2\cdot 2+}$. Propeller geometries are observed for triarylamine moieties, with each nitrogen atom nearly coplanar to three neighboring carbon atoms. The *para*-bridged aryl rings show a quinoidal geometry in comparison to the *meta*-bridged aryl rings.

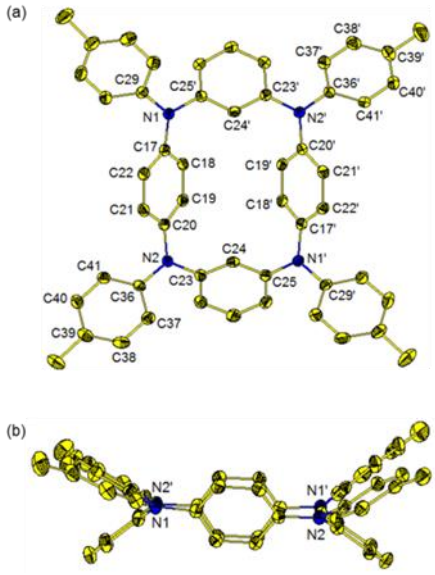

Figure 2. Ortep plots of $\mathbf{1}^{2\cdot 2+}$ (thermal ellipsoids 50%). (a) top view and (b) side view. Hydrogen atoms were omitted for clarity. Selected bond lengths (Å) and angles (deg): N1–C17 1.386(3), N1–C29 1.427(3), N1–C25' 1.433(3), N2–C20 1.385(3), N2–C23 1.427(3), N2–C36 1.431(3), C17–C18 1.415(3), C18–C19 1.364(3), C19–C20 1.408(3), C17–C22 1.405(3), C22–C21 1.372(3), C21–C20 1.416(3), C17–N1–C25' 117.9(1), C17–N1–C29 124.8(1), C25'–N1–C29 117.3(1), C20–N2–C23 119.4(1), C20–N2–C36 122.2(1), C23–N2–C36 118.4(1).

The average N-C bond lengths to the peripheral phenyl ring (1.426 Å) and the *meta*-bridged aryl ring (1.441 Å) are much longer than that to the *para*-bridged phenyl ring (1.382 Å), indicating the electron spin density mainly delocalize on the nitrogen atoms and the *para*-bridged phenyl rings. The distances between the nitrogen atoms are 4.85 Å (N1···N2) and 5.54 Å (N2···N1') on the sides, 7.39 Å (N1···N1') along the diagonal of the rectangle consisting of four nitrogens.

The optimized geometry,[14] together with the geometric parameters, including the N-C and C-C bond lengths, as well as N···N distances, of the calculated $\mathbf{1}^{2\cdot 2+}$ in the triplet ground state is similar to that obtained from the X-ray structure. The singlet-triplet energy gap, $\Delta E_{ST} = 0.9$ kcal mol^{-1}, is calculated.[15] The electron spin density is mainly delocalized on four nitrogen atoms and aryl rings along the rectangle (Table S5, SI and Figure 3), but with considerable spin density on the peripheral phenyl rings.

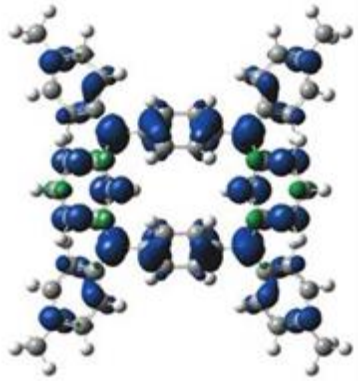

Figure 3. Spin density distribution of the triplet $\mathbf{1}^{2\cdot 2+}$.

Magnetic Studies. Magnetic studies of diradical dication salt $\mathbf{1}^{2\cdot 2+}\cdot 2[Al(OR_{Me})_4]^-$ in the solid state were carried out using SQUID magnetometry. For polycrystalline sample, the χT vs. T (H = 30000 Oe) plot shows a broad maximum at T = 80 K, corresponding to $\chi T \approx 0.9$ emu K mol^{-1}; at the extreme temperatures, T = 350 and 1.85 K, the χT is dropping off to about $\chi T \approx 0.8$ and 0.09 emu K mol^{-1}, respectively (Figure 4A). These data suggest that $\mathbf{1}^{2\cdot 2+}\cdot 2[Al(OR_{Me})_4]^-$ possesses a triplet ground state (S = 1) that is somewhat de-populated at high T (e.g., T = 350 K), i.e., the singlet triplet energy gap $2J/k$ (or ΔE_{ST}) is less than the thermal energy at room temperature ($2J/k$ < 300 K or ΔE_{ST} < 0.6 kcal mol^{-1}).

The singlet triplet energy gap for $\mathbf{1}^{2\cdot 2+}\cdot 2[Al(OR_{Me})_4]^-$ is estimated by numerical fitting of the χT vs. T data in the T = 80 - 350 K range to the diradical model (eq. 1).[5c] The optimized values of the variable parameters are as follows: $2J/k \approx 240$ K, the mean-field correction for an intermolecular antiferromagnetic coupling, θ = -0.4 K, and the weight factor N = 0.92. Thus, experimental $\Delta E_{ST} \approx$ 0.5 kcal mol^{-1} is below the computed value of 0.9 kcal mol^{-1}, as expected for broken symmetry DFT computations.[6j]

$$\chi T = (1.118T/H)N\{2\sinh(a)/[1 + \cosh(a) + \exp((-2J/k)/T)]\} \quad (1)$$

$$a = 1.345(H/(T - \theta))$$

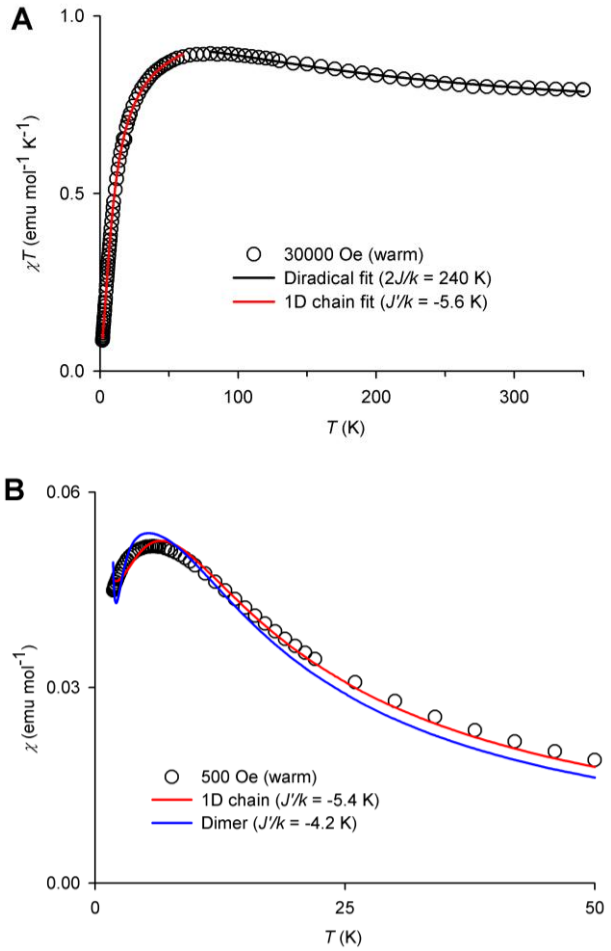

Figure 4. SQUID magnetometry for polycrystalline diradical dication salt $\mathbf{1}^{2\cdot 2+}\cdot 2[Al(OR_{Me})_4]^-$: plot A, χT vs. T at H = 30000 Oe in the warming mode and plot B, χ vs. T at T = 1.8 - 50 K and H = 500 Oe in the warming mode. In each of the numerical fits with three variable parameters, Heisenberg exchange coupling constant, J/k or J'/k, mean-field correction, θ, and weight factor, N, the values of standard error, *SE*, and parameter dependence, *DEP*, are provided. Goodness of fit may be measured by standard error of estimate, *SEE*. Numerical fits for plot A: 80 - 350 K, diradical, J/k = 120 (*SE* = 13, *DEP* = 0.994), N = 0.92 (*SE* = 0.012, *DEP* = 0.997), θ = -0.4 (*SE* = 0.7, *DEP* = 0.971), R^2 = 0.9903, *SEE* = 0.0038; 1D chain (T = 1.8 - 60 K), J'/k = -5.61 (*SE* = 0.04, *DEP* = 0.8948), N = 1.009 (*SE* = 0.002, *DEP* = 0.666), θ = +0.54 (*SE* = 0.03, *DEP* = 0.831), R^2 = 0.9997, *SEE* = 0.0048. Numerical fits for plot B: 1.8 - 50 K, 1D chain, J'/k = -5.4 (*SE* = 0.07, *DEP* = 0.952), N = 1.03 (*SE* = 0.011, *DEP* = 0.921), θ = +0.31 (*SE* = 0.02, *DEP* = 0.807), R^2 = 0.9889, *SEE* = 0.0010; Dimer, J'/k = -4.2 (*SE* = 0.06, *DEP* = 0.951), N = 0.88 (*SE* = 0.014, *DEP* = 0.837), θ = +1.5 (*SE* = 0.02, *DEP* = 0.892), R^2 = 0.9501, *SEE* = 0.0021.

Further confirmation of triplet ground state was obtained by quantitative EPR spectroscopy of $\mathbf{1}^{2\cdot 2+}\cdot 2[Al(OR_{Me})_4]^-$ in dibutylphthalate (DBP) glass.[6j,16] At 117 K, χT = 0.96 ± 0.01 emu K mol^{-1} was obtained by spin counting, which is in a good agreement with $2J/k \approx 240$ K obtained by SQUID magnetometry. The spectrum may be fit to S = 1 diradical with $|D/hc| \approx 5.6 \times 10^{-3}$ cm^{-1} (Figure 6 and Figure S7, SI).

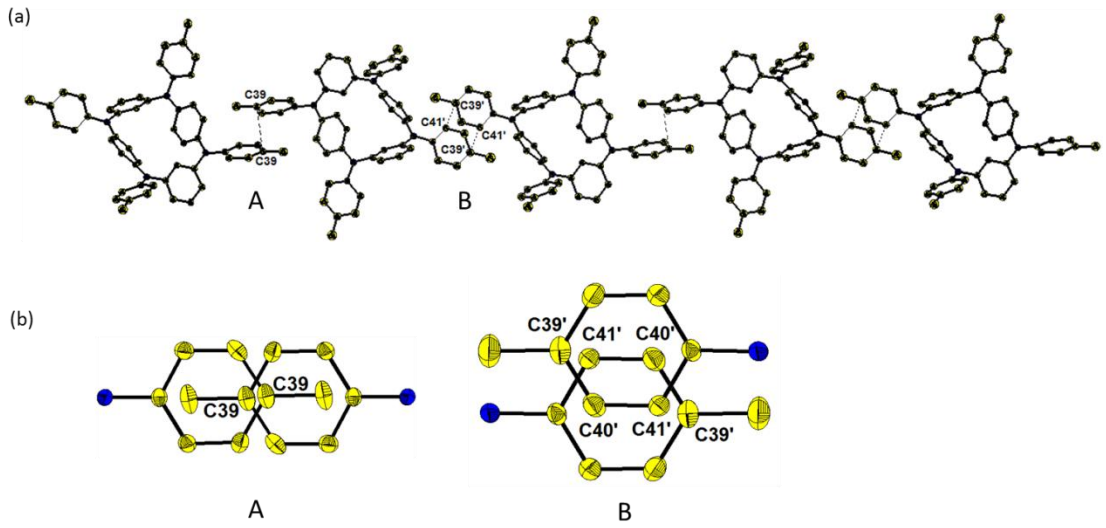

Figure 5. (a) The 1-D antiferromagnetic spin-1 chain with intermolecular C···C interactions (Types A and B) in the crystal structure of diradical dication $\mathbf{1}^{2\cdot 2+}$. (b) Top-views of intermolecular C···C interactions (Types A and B).

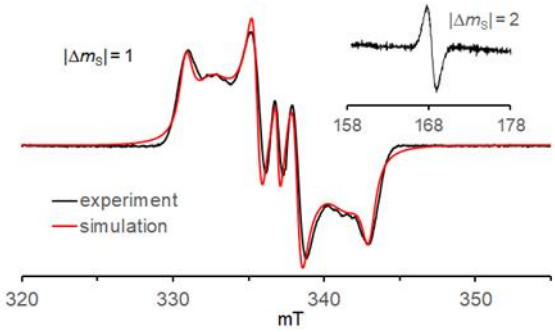

Figure 6. EPR spectrum of $\mathbf{1}^{2\cdot 2+}\cdot 2[Al(OR_{Me})_4]^-$ in DBP glass at 117 K; center line corresponds to small amount of $S = ½$ (monoradical) impurity. Spectral simulation of the $|\Delta m_S| = 1$ region: $S = 1$, $|D/hc| = 5.64 \times 10^{-3}$ cm^{-1}, $|E/hc| \approx 1.03 \times 10^{-3}$ cm^{-1}, $|A_{yy}/hc| \approx 4 \times 10^{-4}$ cm^{-1}, $g_x = 2.0030$, $g_y = 2.0020$, $g_z = 2.0030$; $S = ½$ (center line): $|A_{yy}/hc| \approx 8 \times 10^{-4}$ cm^{-1}, $g_x = 2.0030$, $g_y = 2.0020$, $g_z = 2.0030$. This EPR spectrum together with complete set of simulation and experimental parameters is provided in the SI, Figure S7.

Because $\mathbf{1}^{2\cdot 2+}\cdot 2[Al(OR_{Me})_4]^-$ was determined to possess triplet ground states with moderate ferromagnetic coupling ($2J/k$ = 240 K), the downward turn at low temperatures in the χT vs. T plots must be due to intermolecular antiferromagnetic coupling between S = 1 diradical dication molecules. Indeed, the low temperature section of the χT vs. T plot (T = 1.85 - 60 K) is well fit to the one-dimensional (1-D) antiferromagnetic Heisenberg chain of spin-1 model (Figure 4A, eq. 2).

In the χ vs. T plots, maxima are observed at about 6 K (Figure 4B), which tends to broaden and shift to slightly lower temperature at higher magnetic fields, e.g, H = 30000 Oe (Figure S6, SI). Two limiting models for such intermolecular antiferromagnetic coupling are considered: (1) one-dimensional (1-D) Heisenberg chains of S = 1 diradicals (spin-1 chain) (eq. 2) and (2) pairs of S = 1 diradicals (dimer) (eq. S1, SI). The numerical fits to these models are obtained in the limited temperature range (1.8-50 K), i.e., to ensure that $\mathbf{1}^{2\cdot 2+}$ is almost completely in its S = 1 ground state at the highest temperature (50 K), which is considerably lower than $2J/k \approx 240$ K.

The χ vs. T data provide an excellent fit (coefficient of determination, R^2 = 0.9889, and standard error of estimate, SEE = 0.0010) to a model for a 1-D antiferromagnetic spin-1 chain with three variable parameters: intra-chain antiferromagnetic coupling, J'/k = -5.4 K, the mean-field correction for an inter-chain ferromagnetic coupling, θ = +0.31 K, and a weight factor, N = 1.03 (eq. 2, Figure 4B).[17] This fit is considerably better than the alternative three-parameter fit to pairs of S = 1 diradicals (dimer model) as indicated by the values of R^2 = 0.9501 and SEE = 0.0021 (Figure 4B). This suggests that the dimer model is not suitable for diradical dication salt $\mathbf{1}^{2\cdot 2+}\cdot 2[Al(OR_{Me})_4]^-$ and it is further confirmed by fits using two-parameter models (J'/k and N) (Figures S3-S6, SI).

$$\chi_{1D} = [3/(2k(T - \theta))][(2 + a_1\times K + a_2\times K^2)/(3 + b_1\times K + b_2\times K^2 + b_3\times K^3)] \quad (2)$$

$a_1 = 0.0194$, $a_2 = 0.777$,

$b_1 = 4.346$, $b_2 = 3.232$, $b_3 = 5.634$,

$K = -J'/kT$

Further support for the 1-D antiferromagnetic spin-1 chains is provided by the crystal packing of $\mathbf{1}^{2\cdot 2+}\cdot 2[Al(OR_{Me})_4]^-$, as discussed below. Molecules of $\mathbf{1}^{2\cdot 2+}$ unexpectedly pack into 1-D chains (Figure 5a) along the body diagonal of the unit cell. Two types of short intrachain aryl C···C contacts between the peripheral aryl rings

(A and B in Figure 5 and Table S2, SI) are observed. The distance of the inter-aryl C39···C39 contact (3.556 Å) in type A is close to the van der Waals contact (3.54 Å). In type B, the distance of the inter-aryl C39'···C41' contacts (3.651 Å) are slightly longer, while C40'···C41' contacts (3.515 Å) are shorter than the van der Waals contact. The distance between aryl rings in type B is shorter (3.49 Å), associated with a π-π interaction. Effective exchange coupling pathways through inter-aryl C···C contacts were reported in crystalline dimer of $S = 1$ nitroxide diradicals. For the intrachain C···C contacts in $\mathbf{1}^{2\cdot 2+}$, the carbon atoms (C39, C39' and C41') of the peripheral aryl rings possess considerable large, positive spin density, while the carbon atoms (C40') has relatively smaller, negative spin density (Figure 5, Table S4, SI). These C···C contacts (Table S2, SI) and spin densities are similar in magnitude to those in dimeric $S = 1$ nitronyl nitroxide-substituted 5,10-diphenyl-5,10-dihydrophenazine radical cation, which possessed the inter-aryl C···C contacts (3.566 Å) associated with intermolecular exchange coupling of $J' \approx -18$ K.[6e] Since the interacting atoms in $\mathbf{1}^{2\cdot 2+}$ with positive spin densities are in the nonorthogonal (overlapping) orbitals, the intrachain exchange coupling between $S = 1$ diradical dications is antiferromagnetic. The 1-D chains are separated by the $[Al(OR_{Me})_4]^-$ anions with negligible non-overlapped π-π interaction between chains (Figures S1-2, SI), which may rationalize the weak interchain ferromagnetic exchange coupling. Crystalline diradical dication $\mathbf{1}^{2\cdot 2+}$ thus can be viewed as a 1-D antiferromagnetic spin $S = 1$ chain.

Our magnetic data clearly support 1-D chain of $S = 1$ diradicals and exclude pairs of $S = 1$ diradicals (dimer). We note that the dimer model may be viewed as a 1-D chain with values of J' alternating between J' and zero. To explore whether intra-chain contacts type A and B could provide a significant alternation of J' we set out to compute J' for type A and B, using fixed geometries of X-ray structures at low temperatures. In addition to the X-ray data at 123 K, we determined another structure at 90 K (Table S1, SI). The structures obtained at both temperature are very similar. However, there are important changes in intermolecular (interchain) distance in dimers A and B (Table S2, SI). At 90 K, the type A, C39···C39 (para-para) contacts and type B, C40'···C41' (meta-ortho) contacts becomes only slightly shorter, but the type B, C39'···C41' (para-ortho) contacts becomes considerably shorter (3.651 Å at 123 K vs. 3.602 Å at 90 K). The relatively increased antiferromagnetic interaction in dimer B, compared to that in dimer A, may be thus expected at low temperature.[18] We use the X-ray structures at 123 K and 90 K in the DFT calculations of dimers A and B at the fixed geometries, using the broken symmetry method by Datta and coworkers,[8b,15] to determine the values of J' for the dimer A (J_A) and dimer B (J_B). The computed J' at the UB3LYP/6-311++G(d,p) level for the structure at 123 K are $J_A' = -10.7$ K and $J_B' = -2.4$ K and for the structure at 90 K are $J_A' = -8.7$ K and $J_B' = -1.4$ K (Table S3, SI). The results suggest that difference in values of J_A' and J_B' in the spin-1 chain decreases with temperature. Thus, the values of the alternating J' are likely to become more similar at lower temperatures (1.8 - 50 K range), at which magnetic studies are carried out.[19]

Thermal Stability. We studied thermal stability of $\mathbf{1}^{2\cdot 2+}\cdot 2[Al(OR_{Me})_4]^-$ by thermogravimetric analysis and EPR spectroscopy. TGA profiles under N_2 atmosphere, with parallel analysis of the head space with IR spectroscopy, indicate that the onset of decomposition (1% mass loss) occurs at 182 °C (Figure 7, and Figures S8 and S9, SI). Overlays of the most intense IR spectrum with the IR spectra of hexafluoroacetone and 1,1,1-trifluoroacetone may suggest a mixture of the two ketones, according to qualitative spectral comparison (Figure S11, SI). This may imply that the mass loss in the TGA experiment is associated with decomposition of the counterion. In another TGA/IR experiment, the sample was heated up to 190 °C and then annealed for 10 min. EPR spectra of the solid residue revealed the absence of the diradical dication; a small amount of monoradical (spin concentration of ~5%) was detected (Figure S10, SI).

The onset decomposition temperature at 182 °C for $\mathbf{1}^{2\cdot 2+}\cdot 2[Al(OR_{Me})_4]^-$ may be compared to the onset decomposition at about 175 °C for the recently reported thermally robust neutral triplet ground state diradical with a similar ΔE_{ST}.[6j] The onset decomposition of $\mathbf{1}^{2\cdot 2+}$ on air occurs at only slightly lower temperature of about 170 °C, as confirmed by the EPR spectroscopic follow up of thermally annealed samples of $\mathbf{1}^{2\cdot 2+}\cdot 2[Al(OR_{Me})_4]^-$ (Figure S12, SI).

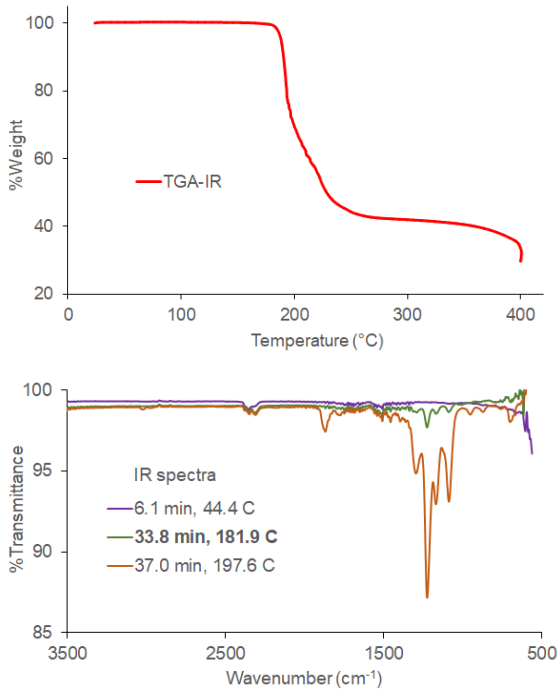

Figure 7. Top plot: TGA for polycrystalline $\mathbf{1}^{2\cdot 2+}\cdot 2[Al(OR_{Me})_4]^-$ under N_2 atmosphere; heating rate = 5 °C min^{-1}. Bottom plots: selected IR spectra of the head space obtained during the TGA; the spectrum at 33.8 min, shown in dark green color, corresponds to an onset of decomposition at temperature of 181.9 °C and with remaining mass of 99.2%. IR spectra acquired during the TGA are summarized in the SI, Figures S9-S11).

CONCLUSION

In summary, diradical dication $\mathbf{1}^{2\cdot 2+}$ possess high thermal stability and a triplet ground state with a moderate $\Delta E_{ST} \approx 0.5$ kcal mol^{-}

[1]. The magnetic behavior for $\mathbf{1}^{2\cdot2+}\cdot2[Al(OR_{Me})_4]^-$ at low temperature is best modeled by 1-D spin $S = 1$ Heisenberg chain with intrachain antiferromagnetic coupling ($J'/k = -5.4$ K) and a small inter-chain ferromagnetic coupling ($\theta \approx 0.3$ K). The intrachain antiferromagnetic coupling is related to a Haldane gap of $0.41 \times 2|J'/k| \approx 4.4$ K and highly isotropic chains with weak local anisotropy, $|D/2J'| \approx 7 \times 10^{-4}$; high isotropicity is notable as the local anisotropy is about three orders of magnitude smaller than the local anisotropy ($|D/2J'| = 0.2-0.3$) found in the most studied Ni(II)-based spin-1 chains such as NENP and NDMAP.[4f] For $\mathbf{1}^{2\cdot2+}\cdot2[Al(OR_{Me})_4]^-$, the estimated Haldane gap and local $S = 1$ anisotropy are greater by factor of two and smaller by an order of magnitude, respectively, compared to those in the previously reported nitroxide diradicals.[8] The antiferromagnetic coupling between the $S = 1$ diradicals is ascribed to the aryl C···C contacts, including π-π interactions. The work provides a novel system for studies of low dimensional magnetism, and search for related 1-D chains is underway.

EXPERIMENTAL SECTION

All experiments were carried out under a nitrogen atmosphere by using standard Schlenk and glove box techniques. Solvents were dried prior to use. All palladium-catalyzed reactions were manipulated in the glove box in sealed reaction vessels. $Ag[Al(OR_{Me})_4]$ ($OR_{Me} = OC(CF_3)_2Me$)[12] and $\mathbf{1}$[9a] were synthesized according to the literature procedures. $Pd(OAc)_2$ and $Pd(dba)_2$ were purchased from TCI and used upon arrival. 1,4-Dibromobenzene, 1,3-dibromobenzene and DPPF were used as received from Energy Chemical. Element analysis of $\mathbf{1}^{2\cdot2+}\cdot2[Al(OR_{Me})_4]^-$ was performed at Shanghai Institute of Organic Chemistry, the Chinese Academy of Sciences. The frozen solution EPR spectra were obtained using a Bruker EMX-plus X-band spectrometer and simulated with the WINEPR SimFonia software. TGA instrument (TA Instruments TGA 550) was run either without or with IR attachment (Thermo NICOLET Is50 NIR). Magnetic measurements of $\mathbf{1}^{2\cdot2+}\cdot2[Al(OR_{Me})_4]^-$ were performed using a Quantum Design SQUID VSM magnetometer with fields of 30 000, 5000 and 500 Oe (T = 1.85 – 350 K). Identical sequences of measurements of $\mathbf{1}$, $Li[Al(OR_{Me})_4]$ and film were carried out for the point-by-point correction for diamagnetism.

Synthesis of $\mathbf{1}^{2\cdot2+}\cdot2[Al(OR_{Me})_4]^-$: CH_2Cl_2 (~50 mL) was added to the mixture of $\mathbf{1}$ (0.11 g, 0.15 mmol) and $Ag[Al(OR_{Me})_4]$ (0.26 g, 0.30 mmol) dropwise at room temperature while stirring. Stirring was maintained at room temperature for 1 d. The resultant brown solution was filtered to remove the gray precipitate (Ag metal). The filtrate was concentrated to ~5 ml and appropriate amount of hexane (~4 ml) was added. The solution was then stored at -20 °C for 24 h to afford crystals of $\mathbf{1}^{2\cdot2+}\cdot2[Al(OR_{Me})_4]^-$ that are suitable for single crystal X-ray crystallography. Isolated yield: 0.14 g, 30%; Elemental analysis calcd for $C_{84}H_{68}Al_2F_{48}N_4O_8$ (%): C 45.30, H 3.08, N 2.52; found: C 45.40, H 3.22, N 2.87.

X-ray Crystallographic Data Collection. Crystals of $\mathbf{1}^{2\cdot2+}\cdot2[Al(OR_{Me})_4]^-$ were removed from a Schlenk flask under N_2 and immediately dipped into hydrocarbon oil. A crystal suitable for X-ray diffraction was selected and attached to a glass fiber on a copper pin and rapidly placed in the cold N_2 stream of the diffractometer. X-ray data were collected on a Bruker APEX DUO CCD diffractometer with Mo Kα radiation ($\lambda = 0.71073$ Å) at 123 K or at 90 K. Integrations were performed with SAINT.[20] Absorption corrections were carried out using SADABS program.[21] Crystal structures were solved by direct methods and refined by full-matrix least-squares based on F^2 using the SHELXTL program.[22] All non-hydrogen atoms were refined anisotropically. Details of the data collections and refinements are given in Table S1, SI.

Computational Details. All the geometry optimizations were carried out at the UB3LYP/6-31G(d) level of theory. The obtained stationary points were characterized by frequency calculations. The broken-symmetry approach was applied for open-shell singlet calculations and spin contamination errors were corrected by approximate spin-projection method.[15] Computations of an intrachain coupling constant J' were carried out using dimers A and B (tetraradical tetracations) at both X-ray geometries (123 and 90 K); DFT broken symmetry approach, as implemented by Datta and coworkers, was used (SI).[8b] All calculations were performed with the Gaussian 09 program suite.[14]

ASSOCIATED CONTENT

Supporting Information. Crystallographic data in CIF format, crystal packing, TGA, IR and EPR spectroscopy, theoretical calculations and SQUID magnetic studies. This material is available free of charge via the Internet at http://pubs.acs.org.

AUTHOR INFORMATION

Corresponding Author

xpwang@nju.edu.cn (XW)
arajca1@unl.edu (AR)

Author Contributions

The manuscript was written through contributions of all authors. / All authors have given approval to the final version of the manuscript. /

Notes

The authors declare no competing financial interests.

ACKNOWLEDGMENT

We thank the National Key R&D Program of China (Grant 2016YFA0300404 X.W.), the National Natural Science Foundation of China (Grants 21525102, 21690062 X.W.) and US National Science Foundation (CHE-1665256, A.R.) for financial support. We are grateful to the High Performance Computing Center of Nanjing University for doing the numerical calculations in this paper on its IBM Blade cluster system.

REFERENCES

(1) (a) Landee, C. P.; Turnbull, M. M. Review: A gentle introduction to magnetism: units, fields, theory, and experiment. *J. Coord. Chem.* **2014**, *67*, 375-439. (b) Wierschem, K.; Sengupta, P. Characterizing the Haldane

phase in quasi-one-dimensional spin-1 Heisenberg antiferromagnets. *Mod. Phys. Lett. B* **2014**, *28*, 1430017-1-21.

(2) (a) Haldane, F. D. M. Nonlinear field theory of large-spin Heisenberg antiferromagnets: semiclassically quantized solitons of the one-dimensional easy-axis néel state. *Phys. Rev. Lett.* **1983**, *50*, 1153-1156. (b) Haldane, F. D. M. Continuum dynamics of the 1-D Heisenberg antiferromagnet: identification with the O(3) nonlinear sigma model. *Phys. Lett. A* **1983**, *93*, 464-468.

(3) Selected references: (a) Botet, R.; Jullien, R. Ground-state properties of a spin-1 antiferromagnetic chain. *Phys. Rev. B* **1983**, *27*, 613-615. (b) Sakai, T.; Takahashi, M. Effect of the Haldane gap on quasi-one-dimensional systems *Phys. Rev. B* **1990**, *42*, 4537-4543. (c) Golinelli, O.; Jolicoeur, Th.; Lacaze, R. Haldane gaps in a spin-1 Heisenberg chain with easy-plane single-ion anisotropy. *Phys. Rev. B* **1992**, *45*, 9798-9805. (d) Kim, Y. J.; Birgeneau, R. J. Monte Carlo study of the $S = 1/2$ and $S = 1$ Heisenberg antiferromagnet on a spatially anisotropic square lattice. *Phys. Rev. B* **2000**, *62*, 6378-6384. (e) Matsumoto, M.; Yasuda, C.; Todo, S.; Takayama, H. Ground-state phase diagram of quantum Heisenberg antiferromagnets on the anisotropic dimerized square lattice. *Phys. Rev. B* **2001**, *65*, 014407-1-8. (f) Albuquerque, A. F.; Hamer, C. J.; Oitmaa, J. Quantum phase diagram and excitations for the one-dimensional $S = 1$ Heisenberg antiferromagnet with single-ion anisotropy. *Phys. Rev. B* **2009**, *79*, 054412-1-8. (g) Hu, S.; Normand, B.; Wang, X.; Yu, L. Accurate determination of the Gaussian transition in spin-1 chains with single-ion anisotropy. *Phys. Rev. B* **2011**, *84*, 220402-1-4. (h) Moukouri, S.; Eidelstein, E. Universality class of the Mott transition in two dimensions. *Phys. Rev. B* **2012**, *86*, 155112-1-8. (i) Wierschem, K.; Sengupta, P. Quenching the haldane gap in spin-1 Heisenberg antiferromagnets. *Phys. Rev. Lett.* **2014**, *112*, 247203-1-5.

(4) Selected examples: (a) Mutka, H.; Payen, C.; Molinié, P.; Soubeyroux, J. L.; Colombet, P.; Taylor, A. D. Dynamic structure factor [$S(Q, \omega)$] of the $S = 1$ quasi-one-dimensional Heisenberg antiferromagnet: neutron-scattering study on $AgVP_2S_6$. *Phys. Rev. Lett.* **1991**, *67*, 497-500. (b) Gadet, V.; Verdaguer, M.; Briois, V.; Gleizes, A.; Renard, J. P.; Beauvillain, P.; Chappert, C.; Goto, T.; Le Dang, K.; Veillet, P. Structural and magnetic properties of $(CH_3)_4NNi(NO_2)_3$: A Haldane-gap system. *Phys. Rev. B* **1991**, *44*, 705-712. (c) Takigawa, M.; Asano, T.; Ajiro, Y.; Mekata, M.; Uemura, Y. J. Dynamics in the $S = 1$ One-dimensional antiferromagnet $AgVP_2S_6$ via ^{31}P and ^{51}V NMR. *Phys. Rev. Lett.* **1996**, *76*, 2173-2176. (d) Zaliznyak, I. A.; Dender, D. C.; Broholm, C.; Reich, D. H. Tuning the spin Hamiltonian of $Ni(C_2H_8N_2)_2NO_2ClO_4$ by external pressure: A neutron-scattering study. *Phys. Rev. B* **1998**, *57*, 5200-5204. (e) Uchiyama, Y.; Sasago, Y.; Tsukada, I.; Uchinokura, K.; Zheludev, A.; Hayashi, T.; Miura, N.; Böni, P. Spin-vacancy-induced long-range order in a new Haldane-gap antiferromagnet. *Phys. Rev. Lett.* **1999**, *83*, 632-635. (f) Zheludev, A.; Chen, Y.; Broholm, C. L.; Honda, Z.; Katsumata, K. Haldane-gap excitations in the low-Hcone-dimensional quantum antiferromagnet $Ni(C_5D_{14}N_2)_2N_3(PF_6)$. *Phys. Rev. B* **2001**, *63*, 104410-1-5. (g) Zaliznyak, I. A.; Lee, S. H.; Petrov, S. V. Continuum in the spin-excitation spectrum of a haldane chain observed by neutron scattering in $CsNiCl_3$. *Phys. Rev. Lett.* **2001**, *87*, 017202-1-4. (h) Zheludev, A.; Honda, Z.; Chen, Y.; Broholm, C. L.; Katsumata, K.; Shapiro, S. M. Quasielastic neutron scattering in the high-field phase of a Haldane antiferromagnet. *Phys. Rev. Lett.* **2002**, *88*, 077206-1-4. (i) Tsujii, H.; Honda, Z.; Andraka, B.; Katsumata, K. High-field phase diagram of the Haldane-gap antiferromagnet $Ni(C_5H_{14}N_2)_2N_3(PF_6)$. *Phys. Rev. B* **2005**, *71*, 014426-1-6. (j) Bera, A. K.; Lake, B.; Islam, A. T. M. N.; Klemke, B.; Faulhaber, E.; Law, J. M. Field-induced magnetic ordering and single-ion anisotropy in the quasi-one-dimensional Haldane chain compound $SrNi_2V_2O_8$: A single-crystal investigation. *Phys. Rev. B* **2013**, *87*, 224423-1-10.

(5) (a) Salem, L.; Rowland, C. The electronic properties of diradicals. *Angew. Chem., Int. Ed.* **1972**, *11*, 92-111. (b) *Diradicals*, ed. Borden, W. T. Wiley, New York, **1982**. (c) Rajca, A. Organic diradicals and poiyradicais: from spin coupling to magnetism? *Chem. Rev.* **1994**, *94*, 871-893. (d) Breher, F. Stretching bonds in main group element compounds—Borderlines between biradicals and closed-shell species. *Coord. Chem. Rev.* **2007**, *251*, 1007-1043. (e) Martin, D.; Soleilhavoup, M.; Bertrand, G. Stable singlet carbenes as mimics for transition metal centers. *Chem. Sci.* **2011**, *2*, 389-399. (f) Abe, M.; Ye, J.; Mishima, M. The chemistry of localized singlet 1,3-diradicals (biradicals): from putative intermediates to persistent species and unusual molecules with a π-single bonded character. *Chem. Soc. Rev.* **2012**, *41*, 3808-3820. (g) Casado, J.; Ortiz, R. P.; Navarrete, J. T. L. Quinoidal oligothiophenes: new properties behind an unconventional electronic structure. *Chem. Soc. Rev.* **2012**, *41*, 5672-5686. (h) Abe, M. Diradicals. *Chem. Rev.* **2013**, *113*, 7011-7088. (i) Zeng, Z.; Shi, X.; Chi, C.; López Navarrete, J. T.; Casado, J.; Wu, J. Pro-aromatic and anti-aromatic π-conjugated molecules: an irresistible wish to be diradicals. *Chem. Soc. Rev.* **2015**, *44*, 6578-6596. (j) Wingate, A. J.; Boudouris, B. W. Recent advances in the syntheses of radical-containing macromolecules. *J. Polym. Sci., Part A: Polym. Chem.* **2016**, *54*, 1875-1894.

(6) (a) Rassat, A.; Sieveking, H. U. A stable aromatic diradical with strong dipolar electronic interaction. *Angew. Chem., Int. Ed.* **1972**, *11*, 303-304. (b) Veciana, J.; Rovira, C.; Crespo, M. I.; Armet, O.; Domingo, V. M.; Palacio, F. Stable polyradicals with high-spin ground states. 1. synthesis, separation, and magnetic characterization of the stereoisomers of 2,4,5,6-tetrachloro-α,α,α',α'-tetrakis(pentachlorophenyl)-m-xylylene. *J. Am. Chem. Soc.* **1991**, *113*, 2552-2561. (c) Inoue, K.; Iwamura, H. 2-[*p*-(N-tert-butyl-N-oxyamino)phenyl]-4,4,5,5-tetramethyl-4,5-dihydroimidazol-3-oxide-l-oxyl, a stable diradical with a triplet ground state. *Angew. Chem., Int. Ed.* **1995**, *34*, 927-928. (d) Shultz, D. A.; Fico, R. M.; Lee, H.; Kampf, J. W.; Kirschbaum, K.; Pinkerton, A. A.; Boyle, P. D. Mechanisms of exchange modulation in trimethylenemethane-type biradicals: The roles of conformation and spin density. *J. Am. Chem. Soc.* **2003**, *125*, 15426-15432. (e) Hiraoka, S.; Okamoto, T.; Kozaki, M.; Shiomi, D.; Sato, K.; Takui, T.; Okada, K. A stable radical-substituted radical cation with strongly ferromagnetic interaction: nitronyl nitroxide-substituted 5,10-diphenyl-5,10-dihydrophenazine Radical Cation. *J. Am. Chem. Soc.* **2004**, *126*, 58-59. (f) Fukuzaki, E.; Nishide, H. Room-temperature high-spin organic single molecule: nanometer-sized and hyperbranched poly[1,2,(4)-phenylenevinyleneanisylaminium]. *J. Am. Chem. Soc.* **2006**, *128*, 996-1001. (g) Rajca, A.; Shiraishi, K.; Rajca, S. Stable diarylnitroxide diradical with triplet ground state. *Chem. Commun.* **2009**, 4372-4374. (h) Boratynski, P. J.; Pink, M.; Rajca, S.; Rajca, A. Isolation of the triplet ground state aminyl diradical. *Angew. Chem., Int. Ed.* **2010**, *49*, 5459-5462. (i) Suzuki, S.; Furui, T.; Kuratsu, M.; Kozaki, M.; Shiomi, D.; Sato, K.; Takui, T.; Okada, K. Nitroxide-substituted nitronyl nitroxide and iminonitroxide. *J. Am. Chem. Soc.* **2010**, *132*, 15908-15910. (j) Gallagher, N. M.; Bauer, J. J.; Pink, M.; Rajca, S.; Rajca, A. High-spin organic diradical with robust stability. *J. Am. Chem. Soc.* **2016**, *138*, 9377-9380.

(7) (a) Kurata, R.; Sakamaki, D.; Ito, A. Tetraaza[1.1.1.1]*m,p,m,p*-cyclophane diradical dications revisited: tuning spin states by confronted arenes. *Org. Lett.* **2017**, *19*, 3115-3118. (b) Wang, W.; Wang, L.; Chen, S.; Yang, W.; Zhang, Z.; Wang, X. Air-stable diradical dications with ferromagnetic interaction exceeding the thermal energy at room temperature: from a monomer to a dimer. *Sci. China. Chem.* **2018**, *61*, 300-305.

(8) (a) Rajca, A.; Takahashi, M.; Pink, M.; Spagnol, G.; Rajca, S. Conformationally constrained, stable, triplet ground state ($S = 1$) nitroxide diradicals. antiferromagnetic chains of ($S = 1$) diradicals. *J. Am. Chem. Soc.* **2007**, *129*, 10159-10170. (b) Sadhukhan, T.; Hansda, S.; Latif, I. A.; Datta, S. N. Metaphenylene-Based Nitroxide Diradicals: A Protocol To Calculate Intermolecular Coupling Constant in a One-Dimensional Chain. *J. Phys. Chem. A* **2013**, *117*, 13151-13160.

(9) (a) Hauck, S. I.; Lakshmi, K. V.; Hartwig, J. F. Tetraazacyclophanes by palladium-catalyzed aromatic amination. geometrically defined, stable,

high-spin diradicals. *Org. Lett.* **1999**, *1*, 2057-2060. (b) Ito, A.; Ono, Y; Tanaka, K. The tetraaza[1.1.1.1]*m*,*p*,*m*,*p*-cyclophane dication: a triplet diradical having two *m*-phenylenediamine radical cations linked by twisted benzenes. *Angew. Chem.; Int. Ed.*, **2000**, *39*, 1072-1075.

(10) (a) Ito, A.; Tanaka, K. Macrocyclic oligoarylamine-based spin system. *Pure Appl. Chem.*, **2010**, *82*, 979-989. (b) Ito, A. Macrocyclic oligoarylamines as hole- and spin-containing scaffolds for molecule-based electronics. *J. Mater. Chem. C*, **2016**, *4*, 4614-4625.

(11) (a) Tan, G.; Wang, X. Isolable bis(triarylamine) dications: analogues of Thiele's, Chichibabin's, and Muller's hydrocarbons. *Acc. Chem. Res.*, **2017**, *50*, 1997-2006. (b) Zheng, X.; Wang, X.; Qiu, Y.; Li, Y.; Zhou, C.; Sui, Y.; Li, Y.; Ma, J.; Wang, X. One-electron oxidation of an organic molecule by $B(C_6F_5)_3$; isolation and structures of stable non-para-substituted triarylamine cation radical and bis(triarylamine) dication diradicaloid. *J. Am. Chem. Soc.* **2013**, *135*, 14912-14915. (c) Su, Y.; Wang, X.; Zheng, X.; Zhang, Z.; Song, Y.; Sui, Y.; Li, Y.; Wang, X. Tuning ground states of bis(triarylamine) dications: from a closed-shell singlet to a diradicaloid with an excited triplet state. *Angew. Chem., Int. Ed.* **2014**, *53*, 2857-2861. **2014**, *126*, 2901-2905. (d) Su, Y.; Wang, X.; Li, Y.; Song, Y.; Sui, Y.; Wang, X. Nitrogen analogues of Thiele's hydrocarbon. *Angew.Chem., Int. Ed.* **2015**, *54*, 1634-1637. (e) Li, T.; Tan, G.; Shao, D.; Li, J.; Zhang, Z.; Song, Y.; Sui, Y.; Chen, S.; Fang, Y.; Wang, X. Magnetic bistability in a discrete organic radical. *J. Am. Chem. Soc.* **2016**, *138*, 10092-10095. (f) Su, Y.; Wang, X.; Zhang, Z.; Wang, L.; Wang, X.; Song, Y.; Power, P. P. Thermally controlling the singlet-triplet energy gap of a diradical in the solid state. *Chem. Sci.* **2016**, *7*, 6514-6518. (g) Li, T.; Wei, H.; Zhang, Z.; Zhao, Y.; Sui, Y.; Wang, X. One-dimensional alkylate-bridged Würster's blue-based diradical dications. *Sci. China. Chem.* **2017**, *60*, 602-606.

(12) Krossing, I. The facile preparation of weakly coordinating anions: structure and characterisation of silverpolyfluoroalkoxyaluminates $AgAl(OR_F)_4$, calculation of the alkoxide ion affinity. *Chem. Eur. J.* **2001**, *7*, 490-502.

(13) X-ray data for $\mathbf{1}^{2\cdot 2+}\cdot 2[Al(OR_{Me})_4]^-$ are listed in Table S1 in the supporting information. CCDC-1816732 (123 K) and 1842168 (90 K) contain the supplementary crystallographic data for this paper. These data can be obtained free of charge from the Cambridge Crystallographic Data Centre via www.ccdc.cam.ac.uk/data_ request /cif.

(14) Frisch, M. J.; et al. *Gaussian 09*, Revision B.01; Gaussian, Inc.: Wallingford, CT, **2010**. See SI for full citation.

(15) (a) Kitagawa, Y.; Saito, T.; Ito, M.; Shoji, M.; Koizumi, K.; Yamanaka, S.; Kawakami, T.; Okumura, M.; Yamaguchi, K. Approximately spin-projected geometry optimization method and its application to di-chromium systems. *Chem. Phys. Lett.* **2007**, *442*, 445-450. (b) Yamaguchi, K.; Jensen, F.; Dorigo, A.; Houk, K. N. A Spin Correction Procedure for Unrestricted Hartree–Fock and Møller–Plesset Wavefunctions for Singlet Diradicals and Polyradicals. *Chem. Phys. Lett.* **1988**, *149*, 537–542.

(16) Olankitwanit, A.; Pink, M.; Rajca, S.; Rajca, A. Synthesis of aza-*m*-xylylene diradicals with large singlet-triplet energy gap and statistical analyses of their EPR spectra. *J. Am. Chem. Soc.* **2014**, *136*, 14277-14288.

(17) Meyer, A.; Gleizes, A.; Girerd, J. J.; Verdaguer, M.; Kahn, O. Crystal structures, magnetic anisotropy properties, and orbital interactions in catena - (μ-nitrito) - bis (ethylenediamine) nickel(II) perchlorate and tri-iodide. *Inorg. Chem.* **1982**, *21*, 1729-1739.

(18) Using the X-ray geometries at 123 and 90 K, the computed spin densities for high-spin (quintet) states of dimers A and B were similar (Table S4, SI).

(19) (a) We thank one of the reviewers for suggesting DFT computations of J' and obtaining another low-temperature X-ray structure. We note that Datta and coworkers (ref 8b) obtained the best qualitative agreement for intra-chain J' at the UB3LYP/6-311++G(d,p) level vs. the experiment for the $S = 1$ nitroxide diradical 1D chains. Nevertheless, it is important to note the uncertainty in reliability of the DFT computations of such small $J' \approx -5$ K, involving π-π interactions, in large, highly charged molecules. Even DFT computations of accurate energies on the order of 1000 K (2 kcal/mol), involved in π-π stacking, are a challenge and it was only recently was solved (e.g., ref 19b). (b) Cho, Y.; Cho, W. J.; Youn, S.; Lee, G.; Singh, N. J.; Kim, K. S. Density Functional Theory Based Study of Molecular Interactions, Recognition, Engineering, and Quantum Transport in π Molecular Systems. *Acc. Chem. Res.* **2014**, *47*, 3321–3330.

(20) *SAINTPLUS: Software Reference Manual*, Version 6.45; Bruker-AXS: Madison, WI, **1997–2003**.

(21) Sheldrick, G. M. *SADABS*; University of Göttingen: Germany, **1996**.

(22) Sheldrick, G. M. *SHELXS-97 and SHELXL-97, Programs for Crystal Structure Analysis*; University of Göttingen: Germany, **1997.**

Insert Table of Contents artwork here